Generalized persistence dynamics for active motion

Francisco J. Sevilla[1,*] and Pavel Castro-Villarreal[2,†]

[1] *Instituto de Física, Universidad Nacional Autónoma de México, Apdo. Postal 20-364, 01000, Ciudad de México, México*

[2] *Facultad de Ciencias en Física y Matemáticas, Universidad Autónoma de Chiapas, Carretera Emiliano Zapata, Km. 8, Rancho San Francisco, 29050 Tuxtla Gutiérrez, Chiapas, México*

We analyse the statistical physics of self-propelled particles from a general theoretical framework that properly describes the most salient characteristics of active motion in arbitrary spatial dimensions. Such a framework is devised in terms of a Smoluchowski-like equation for the probability density of finding a particle at a given position, that carries the Brownian component of the motion due to thermal fluctuations, and the active component due to the intrinsic persistent motion of the particle. The active probability current not only considers the gradient of the probability density at the current time, as in the standard Fick's law, but also the gradient of the probability density at all previous times weighted by a memory function that entails the main features of active motion. We focus in the consequences when the memory function depends only on time and decays as a power law in the short-time regime, and exponentially in the long-time one. In addition, we found analytical expressions for the Intermediate Scattering Function and the time dependence of the mean-squared displacement and the kurtosis.

I. INTRODUCTION

The interest in the transport properties of the so-called *active* or *self-propelled* particles has regrown recently due, on the one hand, to their intrinsic out-of-equilibrium nature, in clear contrast with the commonly Brownian particles (now called *passive*); on the other hand, to the designing of artificial particles that use different phoretic mechanisms to self-propel.

A conspicuous feature of active motion is that it is *persistent*, that is to say, the particle retains its direction of motion during a characteristic period of time. Reduced descriptions of active motion in terms of Fokker-Planck equations for the probability density that depends only on the particle positions, i.e., for which the degrees of freedom that define the direction of motion have been marginalized from the joint probability density of finding a particle at a given position, moving at a given direction of motion, at a given time, leads to the so-called *telegrapher's equation* [1] which emerges as an approximation in the long-time regime. This has been analyzed for a particular model of active motion in Euclidean spaces in two and three dimensions [2, 3], and in two dimensional curved manifolds [4, 5].

Many theoretical frameworks that take into account the persistence of active motion have been considered over the years, nevertheless, two of them have been widely used, the so-called *active Brownian motion* (ABM)[6, 7], for which the persistence of orientation is faded by rotational diffusion, and *run-and-tumble motion* (RTM)[8], for which the persistence of the direction of motion is lost by the instantaneous, temporally uncorrelated tumbling events. In the long-time regime, both frameworks are well-approximated by the the telegrapher's equation for the probability density of finding a particle at position $\boldsymbol{x}$ at time t, $\rho(\boldsymbol{x},t)$, which in d spatial dimensions is given by

$$\frac{\partial^2}{\partial t^2}\rho(\boldsymbol{x},t)+\Gamma\frac{\partial}{\partial t}\rho(\boldsymbol{x},t)=c^2\nabla^2\rho(\boldsymbol{x},t), \tag{1}$$

where Γ^{-1} is the *persistence time* and c the propagation speed. These two quantities are directly related to: i) the inverse of the rotational diffusion coefficient D_R and the particle swimming speed v_0 in the model of ABM if the identifications $\Gamma = d(d-1)D_R$ and $c = v_0$, are made, respectively; and ii) to the inverse of the tumbling rate λ and the particle running speed v_0 in the model of RTM if $\Gamma = d\lambda$ and $c = v_0$, are chosen respectively. The *persistence length*, defined as $\ell_p = c\,\Gamma^{-1}$, characterizes the length scale.

As is well known, the telegrapher's equation interpolates between two limits of description: the wave-equation in the short-time regime and the diffusion equation in the asymptotic limit. The good agreement of the results provided by Eq. (1) to describe active motion in the long-time regime is intuitively clear, and has been discussed before in the case of two-dimensional ABM [9]. In this time regime, persistent motion can be effectively described as the motion of passive Brownian particles diffusing with an effective diffusion coefficient given by c^2/Γ. In contrast, the telegrapher's equation fails to account for a correct description of active motion either in the intermediate- or short-time regime, for which the telegrapher's equation describes a wave-like motion that suffers from some issues as has been pointed out already in Refs. [9, 10], in contrast to the distortionless propagation, in the short-time regime, of a pulse of active particles.

A recent analysis on data acquired from diffusing Janus particles in two dimensions, concluded that it is possible to discern between ABM and RTM by focusing the

* fjsevilla@fisica.unam.mx

† pcastrov@unach.mx

analysis of the Intermediate Scattering Function in the intermediate-time regime [11]. It is therefore of interest to establish generalizations of theoretical frameworks whose validity comprises the whole time regimes to describe active motion, particularly at the intermediate and at the short ones.

In this paper we propose a general theoretical framework based on a Smoluchowski-like equation, to analyse a *generalized active Brownian motion* (GABM) model that incorporates the rather important effects of the persistence of motion through a memory function. This, models the pattern of motion induced by the particular internal mechanism of the particle self-propulsion (this formulation differs of the one considered in Refs. [12, 13], where the internal dynamics of the active particle is embedded in the memory function of the generalized Langevin equation). We consider a memory function whose time dependence takes into account the persistence of motion by slowing down the exponentially decaying memory function, $e^{-\Gamma t}$, that appears in the telegrapher's equation (1) when is rewritten as [14]

$$\frac{\partial}{\partial t}\rho(\boldsymbol{x},t) = c^2 \int_0^t ds\, e^{-\Gamma(t-s)}\, \nabla^2 \rho(\boldsymbol{x},s). \tag{2}$$

Furthermore, our analysis considers the fluctuations exerted by the surroundings and which gives rise to the Brownian component of the particle motion. This allows us for an explicit comparison between the model introduced here and the well-known models of persistent motion active Brownian motion and run-and-tumble motion. Additionally we obtain the explicit time dependence of the mean-squared displacement (MSD) $\langle \boldsymbol{x}^2(t)\rangle$ and of the kurtosis $\kappa(t)$ for the active component of motion.

This paper is organized as follows. In Sec. II the theoretical framework to study the GABM is introduced, within this a generalized telegraphers equation for active motion is presented and analyzed. We provide explicit analytsical expressions for the time dependence of the MSD and the kurtosis ralated to the active part of motion. In Sec. III, we give a comparison between the GABM and the theoretical predictions made by the ABM and RTM models. Finally, in Sec. IV we give our concluding remarks and perspectives.

II. GENERALIZED ACTIVE BROWNIAN MOTION

In this section we provide a novel probabilistic description of the stochastic persistent motion of an active particle, in terms of a transport equation based on the continuity equation

$$\frac{\partial}{\partial t}P(\boldsymbol{x},t) + \nabla\cdot\boldsymbol{J}(\boldsymbol{x},t) = 0, \tag{3}$$

which endows the conservation of probability by coupling the change in time of the probability density function (PDF) $P(\boldsymbol{x},t)$, of finding a particle at the position $\boldsymbol{x}$ at the time t, with the probability current $\boldsymbol{J}(\boldsymbol{x},t)$, which indicates the change of probability per unit of area per unit of time.

The motion of the active particle can be split in two components, each having a different origin. One component comes from the particle's internal mechanisms of self-propulsion and is called active motion, the other component is due to the effects of an external source of stochastic motion, frequently not negligible, like the one provided by a thermal bath which leads to a *passive* component of motion usually referred as Brownian motion. In that case $\boldsymbol{J}(\boldsymbol{x},t)$ can be written as

$$\boldsymbol{J}(\boldsymbol{x},t) = -D_{\mathrm{T}}\nabla P(\boldsymbol{x},t) + \int d\boldsymbol{x}'\, G(\boldsymbol{x}-\boldsymbol{x}',t)\boldsymbol{J}_{\mathrm{a}}(\boldsymbol{x}',t). \tag{4}$$

The first term corresponds to the standard Fick's law with $D_{\mathrm{T}} = k_B T/\gamma$ being the translational diffusion coefficient that characterizes the influence of the surroundings at uniform temperature T; k_B being the Boltzmann constant and γ the friction coefficient that results of the interaction between the particle and the external source of heat, a fluid in most of the cases. $G(\boldsymbol{x}-\boldsymbol{x}',t)$ is the d-dimensional Gaussian distribution, also called the *Brownian propagator*, given by $\exp\{-(\boldsymbol{x}-\boldsymbol{x}')^2/4D_{\mathrm{T}}t\}/(4\pi D_{\mathrm{T}}t)^{d/2}$; and $\boldsymbol{J}_{\mathrm{a}}(\boldsymbol{x},t)$ the contribution to the current due to active motion, which is coupled to the probability density function of active motion, $P_a(\boldsymbol{x},t)$, by the continuity equation

$$\frac{\partial}{\partial t}P_a(\boldsymbol{x},t) + \nabla\cdot\boldsymbol{J}_{\mathrm{a}}(\boldsymbol{x},t) = 0. \tag{5}$$

The physics of Eq. (4) can be understood under the following rationale. The rapid internal dynamics of self-propulsion characterized by the active current $\boldsymbol{J}_a(\boldsymbol{x},t)$, implicitly subordinates the particle's translational dynamics which is also driven by translational fluctuations. Thus, such subordination process is made explicit through the Brownian propagator $G(\boldsymbol{x},t)$, which pulls back the internal dynamics of self-propulsion to the same time-scale of the translational fluctuations taken into account by the Fick's term. In order to determine the statistical properties of the persistent part of motion we require the explicit relation between the current $\boldsymbol{J}_{\mathrm{a}}(\boldsymbol{x},t)$ and the probability density $P_{\mathrm{a}}(\boldsymbol{x},t)$. Here, we assume the generalized form of the Fick's law, namely

$$\boldsymbol{J}_{\mathrm{a}}(\boldsymbol{x},t) = -\nabla\int_0^t dt' K(t,t')P_{\mathrm{a}}(\boldsymbol{x},t'), \tag{6}$$

where $K(t,t')$ denotes a memory function that embeds the implicit dynamics of the particle swimming direction and thus the patterns of active motion. In the cases of physical interest, it can be considered invariant under time translations, i.e. $K(t,t') = K(t-t')$, however in general, such memory can be nonlocal [15] in space too.

Such a complication is unnecessary at the level of description of the present paper. We want to point out in advance that the two first even moments of $P(\boldsymbol{x},t)$ can be written in terms of the memory function $K(t,t')$ [16] as

$$\langle \boldsymbol{x}^2(t)\rangle = 2dD_T t + 2d\int_0^t dt' \int_0^{t'} ds K(t',s), \qquad (7)$$

and

$$\langle \boldsymbol{x}^4(t)\rangle = 4(d+2)\Bigg[D_T\int_0^t ds\langle \boldsymbol{x}^2(s)\rangle + \int_0^t dt'\int_0^{t'} ds K(t',s)\langle \boldsymbol{x}^2(s)\rangle\Bigg]. \qquad (8)$$

On the other hand, active Brownian and run-and-tumble motion provide an explicit stochastic dynamics of self-propulsion, or equivalently, of the pattern of active motion, which in the long-time regime, the details of the fluctuating dynamics of the swimming direction for both models can be cast into the memory function $K(t) = D_{\rm eff}\,\delta(t)$, with $D_{\rm eff}$ an effective diffusion coefficient which is identified with v_0^2/Γ, v_0 being the particle swimming speed and Γ^{-1} the persistence time. A first correction that incorporates the effects of persistence for both models, is given by the exponentially-damped memory function $K(t) = D_{\rm eff}\Gamma\, e^{-\Gamma t}$, which is valid in the long-time regime and leads to the telegrapher's equation (1) after substitution of $K(t)$ in Eq. (5) with $\rho(\boldsymbol{x},t) = P_{\rm a}(\boldsymbol{x},t)$ [14, 17]. Such a memory function can be rigorously obtained in the long-time regime from generic models of active motion, where the polar approximation is valid, i.e. when one can neglect the multipoles of order higher than one in the multipolar expansion of the complete probability density distribution [4, 15, 18] (see appendix B).

In this paper we argue that to fulfill the implicit dynamics of the swimming vector of active particles in the whole span of time, a slow dynamics in the short-time regime should be incorporated into the memory function $K(t,t')$. We propose, instead of the time-translational invariant memory function in (6), an exponentially-damped power-law memory function given explicitly by

$$K(t,t') = c^2\frac{t^{-\eta}e^{-\Gamma t}}{t'^{-\eta}e^{-\Gamma t'}}, \qquad (9)$$

where η is a non-negative dimensionless parameter that takes into account the power law $t^{-\eta}$; c is other parameter with units of speed; and Γ^{-1} as before, is the persistence time. Though (9) is not invariant under time translations, the consequences of such particular form are relevant for the description of active motion as is discussed in the following. Notice that for $\eta = 0$ we recover the exponential memory function that leads to the telegrapher's equation (1).

After substitution of the memory function (9) in Eq. (5), we get a closed equation for the probability density $P_{\rm a}(\boldsymbol{x},t)$, namely

$$\left[\frac{\partial^2}{\partial t^2} + \left(\frac{\eta}{t}+\Gamma\right)\frac{\partial}{\partial t}\right]P_{\rm a}(\boldsymbol{x},t) = c^2\nabla^2 P_{\rm a}(\boldsymbol{x},t). \qquad (10)$$

The second term in the left-hand side of the last expression considers two effects: i) the short-time effects of active motion; and ii) dissipation as occurs in the telegrapher's equation (1), with Γ^{-1} the time-scale that characterizes the correlation time of the orientation of the particle direction of motion. In the dissipationless case, i.e., $\Gamma = 0$, Eq. (10) coincides with the generalization of the wave equation of Bietenholz and Giambiagi [19] in d isotropic spatial dimensions and in $d_\eta = \eta + 1$ isotropic "temporal dimensions". Initial conditions corresponding to a pulse in the origin of coordinates that propagates with vanishing initial flux are of interest and are denoted by $P_{\rm a}(\boldsymbol{x},0) = \delta(\boldsymbol{x})$, and $\partial P_{\rm a}(\boldsymbol{x},0)/\partial t = 0$.

We show that the solutions to the last equation describe active motion in the whole time regime. Furthermore, we show that it improves over the standard approach of getting a hierarchy of coupled equations for the moments of the complete distribution an truncating the hierarchy at some suitable order.

With these considerations we have that the total probability density, $P(\boldsymbol{x},t)$, is then given by the convolution of the Brownian propagator with the probability density of the active part of motion, i.e.,

$$P(\boldsymbol{x},t) = \int d\boldsymbol{x}'\, G(\boldsymbol{x}-\boldsymbol{x}',t)P_{\rm a}(\boldsymbol{x}',t). \qquad (11)$$

A. Probability density function for the effective active motion $P_{\rm a}(\boldsymbol{x},t)$

We can take advantage of the simple physical circumstances considered here, namely, that active particles diffuse freely and isotropically in open space, in order to find solutions to Eq. (10) in Fourier space. After Fourier transforming Eq. (10) we get

$$\frac{d^2}{dt^2}\widetilde{P}_{\rm a}(\boldsymbol{k},t) + \left(\frac{\eta}{t}+\Gamma\right)\frac{d}{dt}\widetilde{P}_{\rm a}(\boldsymbol{k},t) + c^2\boldsymbol{k}^2\widetilde{P}_{\rm a}(\boldsymbol{k},t) = 0, \qquad (12)$$

where we have chosen

$$\widetilde{P}_{\rm a}(\boldsymbol{k},t) = \int d\boldsymbol{x}\, e^{-i\boldsymbol{x}\cdot\boldsymbol{k}}P_{\rm a}(\boldsymbol{x},t) \qquad (13)$$

as the direct Fourier transform, and $\boldsymbol{k}$ denotes the two-dimensional Fourier variable (wave vector) conjugate to $\boldsymbol{x}$. As usual, the inverse transform involves the factor $(2\pi)^{-d}e^{i\boldsymbol{k}\cdot\boldsymbol{x}}$. Equation (12) is complemented by the corresponding initial conditions $\widetilde{P}_{\rm a}(\boldsymbol{k},0) = 1$ and $(\partial/\partial t)\,\widetilde{P}_{\rm a}(\boldsymbol{k},0) = 0$.

The rotational symmetry of Eq. (12) implies that its solution depends only on the magnitude k of $\boldsymbol{k}$, then

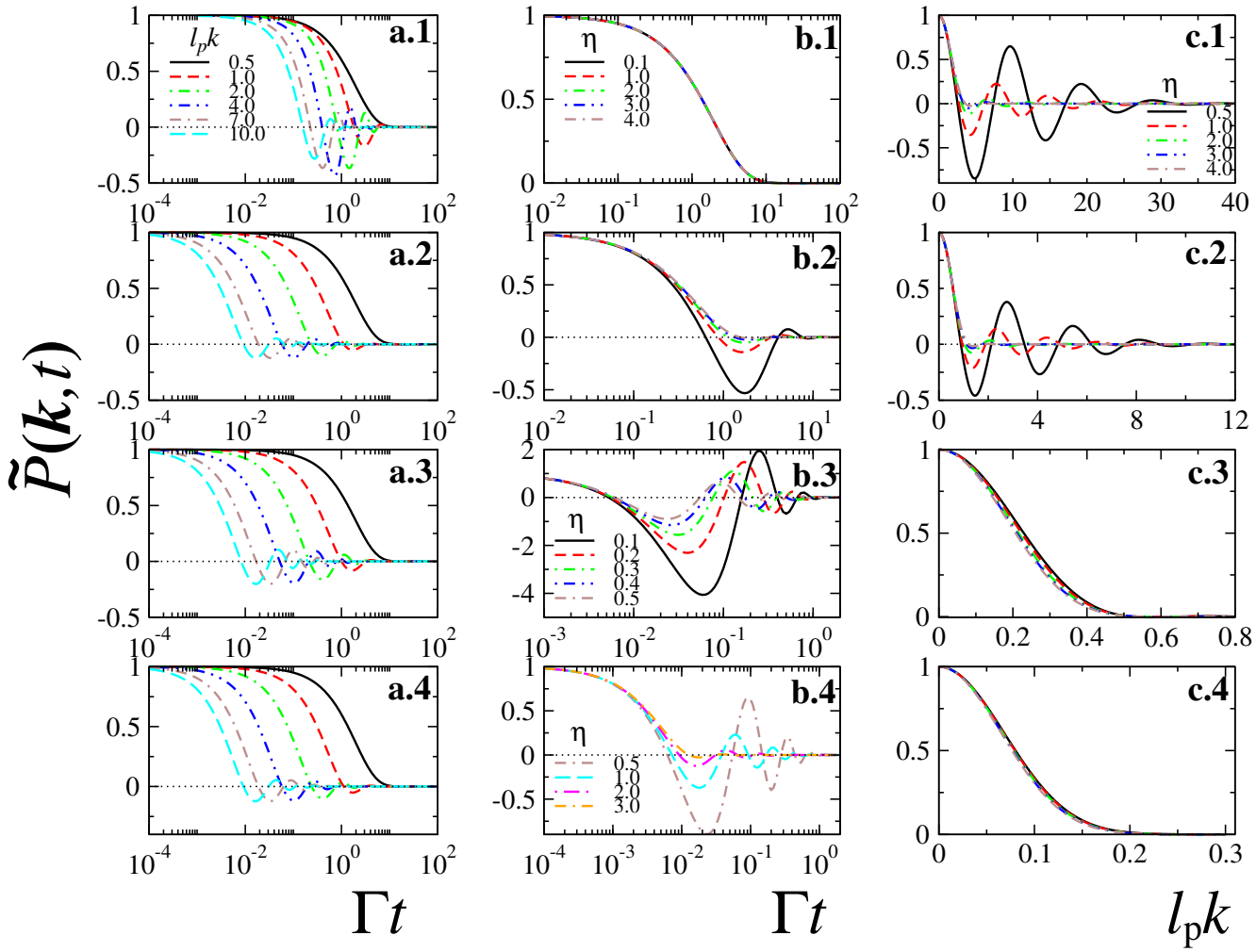

FIG. 1. (Color online) Intermediate scattering function $\widetilde{P}(\boldsymbol{k},t)$ as given in (11) with an inverse Péclet number $\widetilde{D} = D_{\rm T}/\Gamma l_{\rm p}^2 = 0.038$ extracted from the experimental data in Ref. [20]. Columns **a** and **b** as function of the dimensionless time Γt and column **c** as function of the dimensionless wave vector $l_{\rm p}k$. **a.1** $\eta = 0$ **a.2** $\eta = 1$ **a.3** $\eta = 3/2$ **a.4** $\eta = 2$ for different values of the dimensionless wave-vector $l_{\rm p}k$, namely, 0.5, 1 ,2, 4, 7, 10. **b** $l_{\rm p}k$ is fixed for different values of η. **b.1** $l_{\rm p}k = 0.5$; $\eta = 0.1$, 1 , 2, 3 and 4. **b.2** $l_{\rm p}k = 1$ $\eta = 0.1$, 1, 2, 3 and 4. For both panels, **b.3** and **b.4**, $l_{\rm p}k = 10$, with $\eta = 0.1$, 0.2, 0.3, 0.4 and 0.5 for the former panel and $\eta = 0.5$, 1, 2, 3 and 4 for the later. Column **c** shows the dimensionless $\widetilde{P}(\boldsymbol{k},t)$ as function of the dimensionless wave-vector $l_{\rm p}k$ at different times: $\Gamma t = 0.1$ (**c.1**); $\Gamma t = 1.0$ (**c.2**); $\Gamma t = 10.0$ (**c.3**); $\Gamma t = 100.0$ (**c.4**) for different values of η: 0.5, 1.0, 2.0 3.0 4.0.

$\widetilde{P}_{\rm a}(\boldsymbol{k},t) = \widetilde{P}_{\rm a}(k,t)$ and for $\eta \geq 0$ the solution can be written in terms of the Kummer function ${}_1F_1(a,b;z) = \sum_{\ell=0}^{\infty} \frac{(a)_\ell}{(b)_\ell} \frac{z^\ell}{\ell!}$ [21], namely

$$\widetilde{P}_{\rm a}(\boldsymbol{k},t) = e^{-(1+\sigma_k)\Gamma t/2}\, {}_1F_1\left[\frac{\eta}{2}\left(1+\frac{1}{\sigma_k}\right), \eta; \sigma_k\, \Gamma t\right], \tag{14}$$

where $\sigma_k = \sqrt{1-4l_{\rm p}^2k^2}$ is a dimensionless, rotationally invariant function of the dimensionless quantity l_pk.

Thus, the complete probability distribution (11), also known as the *intermediate scattering function* (ISF) [7], is a function of the magnitude of $\boldsymbol{k}$ and is given by

$$\widetilde{P}(\boldsymbol{k},t) = \exp\left\{-t\left[D_{\rm T}k^2 + \frac{\Gamma}{2}(1+\sigma_k)\right]\right\} \times {}_1F_1\left[\frac{\eta}{2}\left(1+\frac{1}{\sigma_k}\right), \eta; \sigma_k\, \Gamma t\right], \tag{15}$$

where the factor $\exp\{-D_{\rm T}k^2t\}$ is the d-dimensional Fourier transform of the Gaussian propagator $G(\boldsymbol{x},t)$ given in (4). The appearance of the dimensionless parameter η and the inverse Péclet number $\widetilde{D}_{\rm T} = D_{\rm T}/(\Gamma l_{\rm p}^2)$ is made explicit in the solution given by (15) when this is written as function of the dimensionless wave vector l_pk.

As it is evident from the expression (15), the behavior is independent of the spatial system dimensionality since the dependence is on the wave-vector magnitude.

The probability density (11), given explicitly in Fourier domain by (15), is shown in Fig. 1 for the reference value of the inverse Péclet number $\widetilde{D}_T = 0.038$ (computed from the data obtained from Janus particles trajectories moving in two dimensions in Ref. [20]), as a function of:

- **a**. The dimensionless time, Γt, for different values of $l_p k$ marked by different line style. The effects of the parameter η are shown in the different panels of the column **a**, namely, **a.1** $\eta = 0$, **a.2** $\eta = 1$, **a.3** $\eta = 3/2$ and **a.4** $\eta = 2$. This behavior is qualitatively similar to the ISF obtained experimentally for Janus particles diffusing in two dimensions [20].

- **b**. The same variable, Γt, for different values of η marked by different line style, at different values of $l_{\rm p} k$ shown in the different panels of the column **b**, that is, **b.1** $l_{\rm p} k = 0.5$, **b.2** $l_{\rm p} k = 1$, both panels **b.3** and **b.4** correspond to $l_{\rm p} k = 10$; notice that the sequence in values of η in **b.4** follows those in **b.3** (the case for $\eta = 0.5$ is repeated in both panels for the sake of a best comparison);

- **c**. The dimensionless magnitude of the wave vector, $l_{\rm p} k$, at the dimensionless time $\Gamma t = 0.1$(**c.1**), 1.0 (**c.2**) for which the characteristic oscillations of active motion are shown, and $\Gamma t = 10$ (**c.3**), $\Gamma t = 100$ (**c.4**), for which the oscillations are damped out and the solutions converge to a universal Gaussian distribution independently of η.

In the short-time regime, $\Gamma t \ll 1$, the damping term (the one proportional to Γ) can be neglected in Eq. (12). In this regime the active probability density for the initial data chosen is given by

$$\widetilde{P}_{\rm a,s\text{-}t}(\boldsymbol{k}, t) \simeq \Gamma\left(d_\eta/2\right) \frac{J_{d_\eta/2-1}(kct)}{(kct/2)^{d_\eta/2-1}}, \qquad (16)$$

where $J_\alpha(z)$ is the α-th order Bessel function of the first kind and we have explicitly shown the dependence on the "temporal dimension" d_η introduced by Bietenholz and Giambiagi in [19]. It is remarkable that Eq. (16) is exactly the same intermediate scattering function of both ABM and RTM when $d_\eta = d$ for each dimension d in the short-time regime [7, 20]. Expression (16) gives rise to a whole family of rotationally symmetric pulses that propagates with speed c, namely

$$P_{\rm a,s\text{-}t}(\boldsymbol{x}, t) = \frac{\Gamma[d_\eta/2]}{2^{d-1}\pi^{d/2}} \int_0^\infty dk\, k^{d-1} \times \frac{J_{d_\eta/2-1}(kct)}{(kct/2)^{d_\eta/2-1}} \frac{J_{d/2-1}(kx)}{(kx/2)^{d/2-1}}, \qquad (17)$$

where it can be noticed that the spatial dimensionality d, and the temporal one d_η, play a symmetric role. In particular, it is noticeable that Eq. (17) reveals a connection between η and the spatial dimensionality of the system d, for if d_η is chosen to be equal to the spatial dimension d, we get that the probability density (16) can be written in the spatial coordinates as the rotationally symmetric sharp pulse:

$$P_{\rm a,s\text{-}t}(\boldsymbol{x}, t) = \frac{\delta(x - ct)}{\Omega_d x^{d-1}}, \qquad (18)$$

which propagates without distortion in any dimension and is free from some of the undesirable features of the propagating pulses given by the wave equation [9], like signal reverberation [22] or negative probabilities [10]. In Eq. (18) $x = |\boldsymbol{x}|$ and $\Omega_d = 2\pi^{d/2}/\Gamma(d/2)$ is the surface of the $(d-1)$-dimensional unit sphere with $\Gamma(z)$ the usual gamma function.

If we take $d_\eta = 1$ in (17), we recover the propagating pulses given by the solutions of the d-dimensional wave equation. As has been pointed out in Refs. [9, 22], such pulses give rise to wake effects, responsible of the anomalous behavior specially in two spatial dimensions where unphysical negative probabilities appear [10]. Notice additionally, that the algebraic decay with distance in (18) differs form the standard decay x^{-1} of the pulse solution of the wave equation in three dimensions.

In the large-time regime, $\Gamma t \gg 1$, we use the approximation ${}_1F_1\left(a, b, z\right) \approx \Gamma[a] e^z z^{a-b}/\Gamma[b]$ for $z \gg 1$ [21], and $\ell_p k \ll 1$ in order to show that the asymptotic expression of the active sector in the intermediate scattering function (15) behaves as

$$\widetilde{P}_{\rm a,l\text{-}t}(\boldsymbol{k}, t) \simeq \exp[-D_{\rm eff} \boldsymbol{k}^2 t]. \qquad (19)$$

This is exactly the same expression of the intermediate scattering function associated to Brownian motion with an effective diffusion constant $D_{\rm eff} = c^2/\Gamma$. It is also remarkable that the three models ABM, RTM and GABM are described by the same ISF (19) at the large-time regime, and this asymptotic expression does not depend on the value of d_η.

B. Mean-squared displacement for the active part of motion

We focus on the mean-squared displacement associated to the effective transport equation (10) proposed here. The contribution to the MSD due to active motion can be obtained directly by calculating the integral in (7) when $D_T = 0$, namely

$$\langle \boldsymbol{x}^2(t) \rangle_{\rm a} = 2d \frac{c^2}{\Gamma} t \Big[1 - {}_2F_2\big(\{1, 1\}, \{2, d_\eta\}, -\Gamma t\big) \Big], \qquad (20)$$

where ${}_2F_2\big(\{a, b\}, \{c, d\}, x\big) = \sum_{n=0} \frac{(a)_n (b)_n}{(c)_n (d)_n} \frac{x^n}{n!}$ is the confluent hypergeometric function [21] and $\langle F(\boldsymbol{x})(t) \rangle_{\rm a}$ denotes the expectation value of $F(\boldsymbol{x})$ calculated with the corresponding probability density of active motion

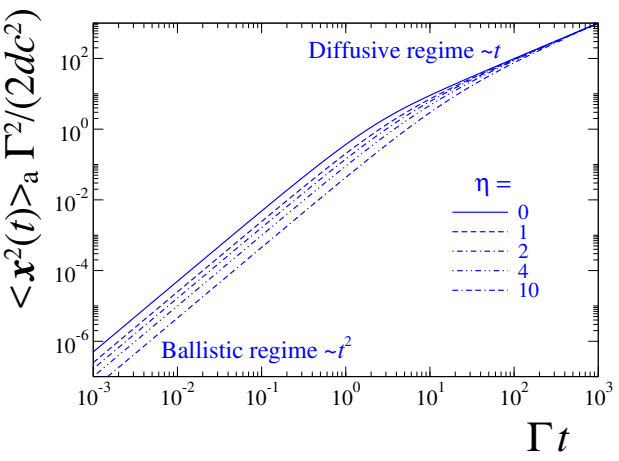

FIG. 2. (Color online) Dimensionless mean square displacement $\left[\Gamma^2/(2dc^2)\right]\langle \boldsymbol{x}^2(t)\rangle_{\rm a}$ as function of the dimensionless time Γt for different values of η. The ballistic behavior, $\sim (d/d_\eta)c^2t^2$ is evident in the short-time regime, while normal diffusion $2dD_{\rm eff}t$ is shown at the long-time regime with $D_{\rm eff}=c^2/\Gamma$.

$P_{\rm a}(\boldsymbol{x},t)$. From the series expansion of the confluent hypergeometric function, the ballistic behavior $\langle \boldsymbol{x}^2(t)\rangle_{\rm a} \simeq v_{\rm eff}^2t^2(1-\frac{2}{3}\frac{\Gamma t}{\eta}+\ldots)$ is evident in the short-time regime $\Gamma t \ll 1$. The effective speed $v_{\rm eff}$, is proportional to c with the proportionality factor given by the square root of the ratio of the spatial dimensionality to the temporal one, i.e., $v_{\rm eff}=\sqrt{d/d_\eta}\,c$. Thus, the proposed model given by (10), give rise to the pulse (17) that propagates with the effective speed $v_{\rm eff}$. If the spatial dimension d is larger than the temporal one d_η the effective speed is larger than c, and the reversed occurs if $d<d_\eta$. As noticed in the previous lines, the case $d_\eta=d$ is of particular interest since the parameter c corresponds precisely to the propagation speed.

By use of the asymptotic behavior of the confluent hypergeometric function in (20), one recovers the diffusive behavior

$$\langle \boldsymbol{x}^2(t)\rangle_{\rm a} = 2dD_{\rm eff}\,t\left\{1+\frac{\eta[\psi(\eta)-\ln\Gamma t]}{\Gamma t}-\frac{\eta(\eta-1)}{(\Gamma t)^2}\times\left[1-\frac{\eta-2}{2\Gamma t}+\frac{(\eta-2)(\eta-3)}{3(\Gamma t)^2}-\ldots\right]\right\}, \quad (21)$$

giving rise to normal diffusion $\sim 2dD_{\rm eff}\,t$ as $\Gamma t\to\infty$, with the diffusion coefficient $D_{\rm eff}=c^2/\Gamma$, where $\psi(x)$ is the digamma function. Notice that although the model makes η to be conspicuously revealed in the short-time regime, it does affect the time dependence of the MSD in the intermediate-time one. To say, while no first correction to the last expression is obtained for $\eta=0$, the linear time dependence of the MSD is corrected by the factor $[1-(\gamma_{\rm e}+\ln\Gamma t)/\Gamma t]$ for $\eta=1$, with $\gamma_{\rm e}\simeq 0.5772\ldots$ the Euler-Mascheroni constant. Higher corrections appear the higher the value of η, these corrections shift the crossover to the diffusive regime to larger times, as is apparent in Fig. 2, where the exact time dependence of the MSD is shown for different values of η. We would like to point out in passing, that an equivalent exact expression for the time dependence of the MSD is given by Eq. (A1) in the appendix A. This expression is obtained directly from (14) using $\langle \boldsymbol{x}^2(t)\rangle_{\rm a}=-\nabla^2_{\boldsymbol{k}}\tilde{P}_{\rm a}(\boldsymbol{k},t)|_{\boldsymbol{k}=0}$, where $\nabla^2_{\boldsymbol{k}}$ is the Laplacian in the Fourier variables.

Specific expressions for the MSD obtained from (20), are given for different values of η in the table I. For $\eta=0$, we recover the well-known expression of persistent motion obtained, among many other equations—as for instance from the Ornstein-Uhlenbeck description of Brownian motion—from the telegrapher's equation. This expression describes the exponentially fast crossover from ballistic motion to normal diffusion, for arbitrary dimension around times of the order of the time scale Γ^{-1}.

TABLE I. Explicit expressions for the mean squared displacement from (20) are given for specific cases of different values of $d_\eta=\eta+1$.

d_η	$\langle \boldsymbol{x}^2(t)\rangle_{\rm a}$
1	$\frac{2dc^2}{\Gamma^2}\left[\Gamma t-\left(1-e^{-\Gamma t}\right)\right]$
2	$\frac{2dc^2}{\Gamma^2}\left[\Gamma t-\mathrm{E_{in}}\left(\Gamma t\right)\right]$,
3	$\frac{2dc^2}{\Gamma^2}\left\{\Gamma t+2\left[1-\mathrm{E_{in}}(\Gamma t)\right]-\frac{2}{\Gamma t}\left(1-e^{-\Gamma t}\right)\right\}$

$\mathrm{E_{in}}(x)=\gamma_{\rm e}+\ln x+\mathrm{E}_1(x)$ where $\mathrm{E}_1(x)=\int_x^\infty dt\,e^{-t}/t$ is the exponential integral function (see Ref. [21]) and $\gamma_{\rm e}\simeq 0.5772\ldots$ the Euler-Mascheroni constant.

C. The Kurtosis $\kappa(t)$ of $P_{\rm a}(\boldsymbol{x},t)$

As it is well known, the kurtosis of a probability density function gives information about its shape. The Kurtosis definition given in Ref. [23], is an invariant measure for multivariate Gaussian distributions and is explicitly given by $\kappa=\left\langle \boldsymbol{x}^T\boldsymbol{\Sigma}^{-1}\boldsymbol{x}\right\rangle$, where $\boldsymbol{x}^T$ denotes the transpose of the d-dimensional vector $\boldsymbol{x}$, and $\boldsymbol{\Sigma}^{-1}$ the so called covariance matrix defined as the inverse of the average for the dyadic product $\boldsymbol{x}\cdot\boldsymbol{x}^T$.

For rotationally-symmetric distributions the kurtosis reduces simply to

$$\kappa(t)=d^2\frac{\left\langle \boldsymbol{x}^4(t)\right\rangle}{\langle \boldsymbol{x}^2(t)\rangle^2}. \quad (22)$$

It can be shown that the kurtosis for a rotationally-symmetric Gaussian distribution with mean $\boldsymbol{\mu}$ and variance σ^2 has the invariant kurtosis value $d(d+2)$. Thus, in the long-time regime it is expected that the kurtosis of the distributions given by (11) and (14) acquire this value, denoted with κ_∞.

An exact expression for the time dependence of $\left\langle \boldsymbol{x}^4(t)\right\rangle_{\rm a}$, suitable to analyze the leading dependence in the short-time regime, is obtained by calculating the integral in (8) when $D_T=0$. Although it is possible to

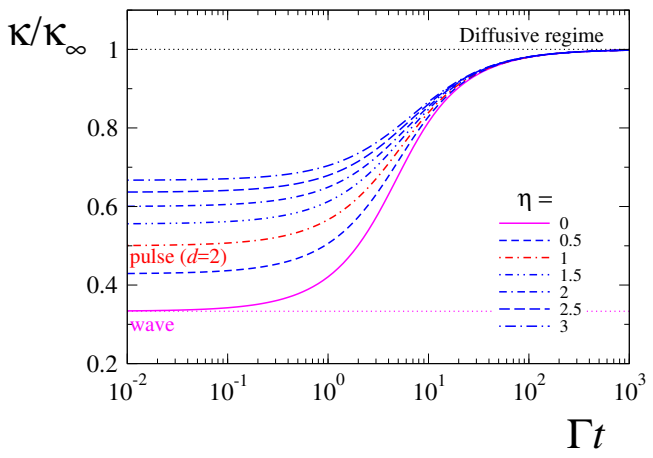

FIG. 3. (Color online) Kurtosis κ/κ_∞ as function of the dimensionless time Γt for different values of the parameter η, where $\kappa_\infty = d(d+2)$ gives the value of the kurtosis for a Gaussian distribution in d spatial dimensions. The dash-dotted line marks the case $\eta = 1$ for which $d_\eta = 2$. The value 0.5 in the short-time limit corresponds to the kurtosis of the pulse given by (18) with $d = 2$.

express it in terms of hypergeometric functions, the following series expansion in power of Γt:

$$\langle \boldsymbol{x}^4(t)\rangle_{\rm a} = 8d(d+2)\eta!(ct)^4 \sum_{n=0}^{\infty} \frac{(-\Gamma t)^n}{(n+\eta+3)!} \times \frac{n+1+\eta\big[\gamma_{\rm e}-1+\psi(n+3)\big]}{n+4}, \quad (23)$$

is more convenient for the sake of analysis in the short-time regime. In this regime the probability density function depends strongly on η, as can be seen from the last expression, since we have for $\Gamma t \ll 1$ that $\langle \boldsymbol{x}^4(t)\rangle_{\rm a} \simeq d(d+2)/((\eta+3)(\eta+1))(ct)^4$; and after dividing this by the mean squared displacement in the same time regime we have that the kurtosis have the η dependent value: $\kappa_{\text{a-str}} \simeq \kappa_\infty(\eta+1)/(\eta+3)$, where $\kappa_\infty = d(d+2)$ and $\kappa_{\text{a-str}}$ denotes the kurtosis $\kappa_a(t)$ of the probability density $P_{\rm a}(\boldsymbol{x},t)$ in the short-time regime. In figure 3, the ratio $\kappa_{\rm a}(t)/\kappa_\infty$, which is independent of the system spatial dimensionality, is shown as function of the dimensionless time Γt for different values of η.

Notice that the value $\eta = 0$ corresponds to the case described by the telegrapher's equation [9] and is characterized by $\kappa_{\text{a-str}}/\kappa_\infty = 1/3$. As noted in Refs. [3, 9], for $d = 2$, and 3, this value describes a wave-like front propagation for which wake effects are present leading to the values $\kappa_{\text{a-str}} = 8/3$ and $\kappa_{\text{a-str}} = 5$ for 2 and three dimensions respectively. Likewise, the connection previously devised between η and the system spatial dimensionality, $\eta = d-1$, which characterizes the shor-time propagating pulse (18), gives $\kappa_{\text{a-str}}/\kappa_\infty = d/(d+2)$, for which the value $1/2$ is obtained for $d = 2$ (see dash-dotted-red line in Fig. 3). Thus, different front propagation are characterized by the ratio $\kappa_{\text{a,s-t}}/\kappa_\infty$. In the long-time regime, the fourth moment of $P_{\rm a}(\boldsymbol{x},t)$, can be obtained alternatively from (14) by use of the formula $\langle \boldsymbol{x}^4(t)\rangle_{\rm a} = \nabla^4_{\boldsymbol{k}} \tilde{P}_{\rm a}(\boldsymbol{k},t)|_{\boldsymbol{k}=0}$ (see appendix A), where $\nabla^4_{\boldsymbol{k}}$ is the bi-Laplacian in the Fourier variables. After a long, but straightforward calculation, one gets the expression (A2) for the fourth moment and from this one, the ratio $\kappa_{\rm a}/\kappa_\infty = 1$, that characterizes the diffusive regime of the probability density distribution is obtained in the lon-time regime (see Fig. 3 upper dotted line).

III. COMPARISON: GENERALIZED ACTIVE BROWNIAN MOTION *VS* ACTIVE BROWNIAN MOTION, AND RUN-AND-TUMBLE MOTION

It is of interest to contrast the results obtained from the model described in section II with those theoretical predictions made for active agents that use the explicit mechanisms of reorientation of the swimming direction of ABM and RTM. Both models can be cast in terms of a transport equation for the probability density function, $P(\boldsymbol{x},\hat{\boldsymbol{v}},t)$, of finding a particle at the point $\boldsymbol{x}$ moving along the direction $\hat{\boldsymbol{v}}$ at the instant t. When the translational motion of the active particle occurs in the d-dimensional Euclidean space, the dynamics of the swimming vector velocity occurs on the surface of the unit $(d-1)$-dimensional sphere S^{d-1}.

The probability density function for active Brownian motion, $P_{\rm ABM}(\boldsymbol{x},\hat{\boldsymbol{v}},t)$, satisfies the Fokker-Planck-like equation

$$\frac{\partial}{\partial t}P_{\rm ABM}(\boldsymbol{x},\hat{\boldsymbol{v}},t) + v_0\hat{\boldsymbol{v}}\cdot\nabla P_{\rm ABM}(\boldsymbol{x},\hat{\boldsymbol{v}},t) = D_{\rm R}\nabla^2_{\hat{\boldsymbol{v}}}P_{\rm ABM}(\boldsymbol{x},\hat{\boldsymbol{v}},t), \quad (24)$$

where $D_{\rm R}$ is the coefficient of rotational diffusion whose inverse, $D_{\rm R}^{-1}$, defines the persistence time; v_0 the particle swimming speed; $\nabla^2_{\hat{\boldsymbol{v}}}$ is the corresponding Laplace-Beltrami operator associated to the unit sphere S^{d-1}, and ∇ is the gradient operator in d spatial dimensions. Analogously, the probability density function for RTM model, $P_{\rm RTM}(\boldsymbol{x},\hat{\boldsymbol{v}},t)$, satisfies the transport equation

$$\frac{\partial}{\partial t}P_{\rm RTM}(\boldsymbol{x},\hat{\boldsymbol{v}},t) + v_0\hat{\boldsymbol{v}}\cdot\nabla P_{\rm RTM}(\boldsymbol{x},\hat{\boldsymbol{v}},t) = -\lambda P_{\rm RTM}(\boldsymbol{x},\hat{\boldsymbol{v}},t) + \lambda\int\frac{d\hat{\boldsymbol{v}}'}{\Omega_d}P_{\rm RTM}(\boldsymbol{x},\hat{\boldsymbol{v}}',t), \quad (25)$$

where the parameter λ is the tumbling rate of the self-propelling particle and $\int d\hat{\boldsymbol{v}}'$ denotes the integration over the d-dimensional unit sphere S^{d-1} and Ω_d its area. A comparison between ABM and RTM has been comprised theoretically to study the many-body effects of active particles that exhibit motility-induced phase separation in the two-dimensions [18]. On the other hand, a comparison between both models against data acquired from

trajectories of Janus particles has been carried out in two dimensions [20], where the authors conclude that the model of active Brownian motion describes better the data analyzed.

Exact analytical expressions for the total intermediate scattering function are known for active Brownian particles freely diffusing in two [20] and three dimensions [7], while the corresponding active intermediate scattering function in one, two and three dimensions for RTM are given in Ref. [8]. Instead of performing a direct comparison between the ISF of ABM and RTM with the one given in this paper in (15), we prefer to make an comparative analysis among the mean-squared displacement and the kurtosis of the active part of the particle's motion. This allows for a more physical analysis of the differences among these patterns of active motion.

For ABM and RTM the mean-squared displacement and the kurtosis are calculated from an analysis based in terms of the hydrodynamic-like tensor fields defined in the appendix B, namely: $\rho(\boldsymbol{x},t)$, the scalar probability density (B1a); $\mathbb{P}^i(\boldsymbol{x},t)$, the i-th component of the polarization vector field (B1b); $\mathbb{Q}^{ij}(\boldsymbol{x},t)$, the elements of the nematic tensor field (B1c); and the elements of the third rank tensor field $\mathbb{R}^{ijk}(\boldsymbol{x},t)$ (B1d).

The procedure presented in the appendix (B) allows us to derive equations for the hydrodynamic-like tensors mentioned above. The conservation of probability leads to the continuity equation, namely

$$\frac{\partial}{\partial t}\rho(\boldsymbol{x},t)+\partial_i J^i(\boldsymbol{x},t)=0, \tag{26}$$

where the i-th component of the probability current, $J^i(\boldsymbol{x},t)$ is given by $v_0\mathbb{P}^i(\boldsymbol{x},t)$ and ∂_i denotes the partial derivative withe respect to the i-th spatial coordinate. Likewise, the evolution equation of the i-th component of the polarization vector $\mathbb{P}^i(\boldsymbol{x},t)$ is

$$\frac{\partial}{\partial t}\mathbb{P}^j=-\xi\,\mathbb{P}^j-\frac{v_0}{d}\partial_j\rho-v_0\partial_k\mathbb{Q}^{jk}, \tag{27}$$

where the parameter ξ acquires the value $(d-1)D_{\rm R}$ for the ABM model, and the value λ for the RTM one, respectively. We note that by combining Eqs. (26) and (27), one get the following inhomogeneous telegrapher's equation

$$\frac{\partial^2}{\partial t^2}\rho+\xi\frac{\partial}{\partial t}\rho=\frac{v_0^2}{d}\nabla^2\rho+v_0^2\partial_i\partial_j\mathbb{Q}^{ij}. \tag{28}$$

On the other hand, the evolution equation for the elements of the nematic tensor $\mathbb{Q}^{ij}$ are given by

$$\frac{\partial}{\partial t}\mathbb{Q}^{ij}=-\overline{\xi}\mathbb{Q}^{ij}-\frac{v_0}{d+2}\mathbb{T}^{ij}-v_0\partial_k\mathbb{R}^{ijk}, \tag{29}$$

with $\mathbb{T}^{ij}=-2\frac{\delta^{ij}}{d}\partial_k\mathbb{P}^k+\partial^i\mathbb{P}^j+\partial^j\mathbb{P}^i$ a second 2-rank traceless tensor field, and the parameter $\overline{\xi}$ acquires the value $2dD_R$ for ABM and the value λ for the RTM, respectively.

Notice that the damping rate in Eq. (27) (first term in the right-hand side) is given by ξ, while it is given by $\overline{\xi}$ in Eq. (29). Thus, $\mathbb{P}^i$ and $\mathbb{Q}^{ij}$ damp out at the same rate for the case of RTM, since $\xi=\overline{\xi}=\lambda$. In contrast, the nematic tensor $\mathbb{Q}^{ij}$ damps out faster than the polarization vector $\mathbb{P}^i$ for ABM, since $\xi>\overline{\xi}$ for $d\geq 2$. It is expected that this occurs also for tensor of higher rank, and therefore this observation precise the difference between both models, in particular this is analyzed by comparison of the time dependence of the kurtosis for each model.

A. The mean-squared displacement and kurtosis

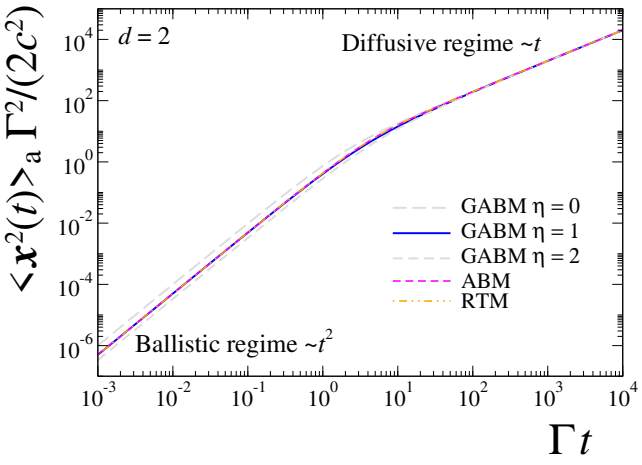

FIG. 4. (Color online) Comparison of the time dependence of mean-squared displacement given by the GABM (20) ($\eta=0$, 1, and 2) and the mean-squared displacement corresponding to ABM and RTM (30), for the two-dimensional case ($d=2$).

The exact time-dependence of the mean-squared displacement for ABM and RTM can be obtained straightforwardly from the inhomogeneous telegrapher's equation [as is shown in the appendix B by use of Eq. (28)] and is given by

$$\langle\boldsymbol{x}^2(t)\rangle=\frac{2v_0^2}{\xi^2}\left[\xi t-(1-e^{-\xi t})\right]. \tag{30}$$

As has been mentioned in Sect. II B, this expression arises from a variety of models of persistent motion, exhibiting the ballistic time dependence $\langle\boldsymbol{x}^2(t)\rangle\simeq v_0^2t^2$, in the short-time regime $\xi t\ll 1$, and the linear time dependence $\langle\boldsymbol{x}^2(t)\rangle\simeq 2dD_{\rm eff}\,t$, in the regime of long times, $\xi t\gg 1$, with $D_{\rm eff}=v_0^2/(d\,\xi)$. For the GABM model presented in this paper, the Eq. (30) arises naturally only for the case $\eta=0$ (see Table I), however, in general, there is no quantitative agreement between the MSD for $\eta=0$ and the expression (30) for constant values of the set of parameters: $\{c,\,\Gamma,\,v_0,\,D_{\rm R}$ and $\lambda\}$ (see the curves for $\eta=0$, long-dashed-gray line, ABM dashed-magenta line and RTM dashed-doble-dotted-orange line in Fig. 4 in two spatial dimensions). A good agreement among

the time dependence of the three models (see the solid-blue line in Fig. 4 for two spatial dimensions and the lines for ABM and RTM) is obtained when the spatial dimensionality, d, plays the same role as the temporal one, i.e., $d_\eta = d$ or equivalently $\eta = d-1$. In addition we must to chose $\Gamma = D_R d(d-1)$ for a proper comparison with ABM and $\Gamma = \lambda d$ to compare with RTM. In both cases we set $c = v_0$. That such is the case can be easily proof by requiring that the moments at both, the short- and long-time regimes of our model, coincide with the corresponding ones of the ABM and RTM.

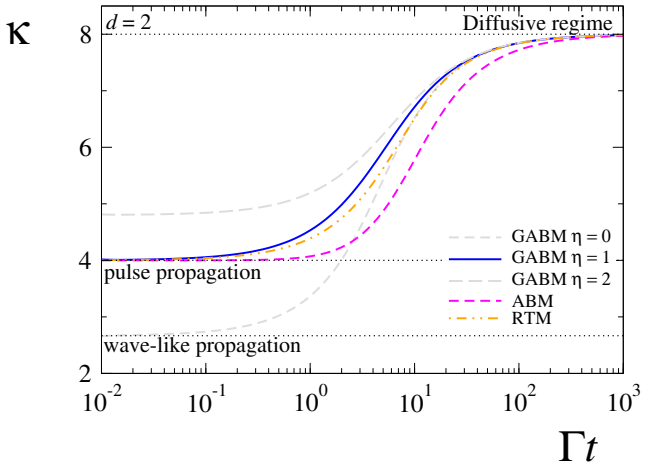

FIG. 5. (Color online) Comparison of the time dependence of the probability distribution kurtosis given by the GABM for $\eta = 0$ (dashed-gray line), 1 (solid-blue line), and 2 (short-dsashed-gray line), and the mean-squared displacement corresponding to ABM and RTM (30), for the two-dimensional case ($d = 2$).

We want to point out that even when the agreement in the mean squared displacement is good, the position distribution reveals differences among the three patterns of active motion considered, as is revealed in the intermediate-time regime of the kurtosis shown in Fig. 5, which for the time-scales chosen, the GABM grows more rapidly than ABM and RTM. There, it can be noticed that in the short-time regime, the case for which $\eta = 1$, properly describes the distorsionless pulse propagation (characterized by $\kappa = 4$ in two spatial dimensions) exhibited by ABM and RTM in contrast to the case $\eta = 0$, which gives rise to wake effects of wave-like propagation characterized by $\kappa = 8/3 \simeq 2.667$ in two spatial dimensions [9]. In the long-time the kurtosis of the three distributions reach the value 8 that univocally characterizes the Gaussian distribution of normal diffusion.

IV. CONCLUDING REMARKS AND PERSPECTIVES

In this paper, we proposed and studied a novel model for active motion that incorporates the persistent effects through the memory function (9). The specific choice of such function implies the Smoluchowski-like equation (10), for the probability density function, $P_{\rm a}(\boldsymbol{x}, t)$, of finding a particle at the position $\boldsymbol{x}$ at the time t in a d-dimensional space; this density function entails the information of the activity. The main feature of the kernel memory is that it is damped out slower than the corresponding telegrapher's one [14, 17] in the short-time regime, leading to an original generalization of the well-known telegrapher's equation characterized by the parameter η. Our analysis takes into account the fluctuations of a thermal bath as well. The joint effect of thermal and active fluctuations is encompassed in the total probability density function $P(\boldsymbol{x}, t)$, given by Eq. (11), whose Fourier transform give us the intermediate scattering function (see Eq. (15)). Thus our analysis avoids the sometimes cumbersome hierarchy analysis made for active Brownian and run-and-tumble motion and allows a qualitative comparison with the experimental data for Janus particles [20].

We also have presented an analysis of the time dependence of the mean-squared displacement and of the kurtosis of the particle position distribution, and we studied the deep consequences of the memory parameter η. To be explicit, we uncovered a large class of active-motion patterns that propagates distinctly as the parameter η is varied, when $\eta = d-1$ it manifestly captures the dynamics of active Brownian motion and run-and-tumble motion at the short- and long- time regimes, if the relations $\Gamma = D_R d(d-1)$ and $\Gamma = \lambda d$ are satisfied. In the intermediate-time regime however, we show that there is not apparent difference among the three models if one is focused only in the time-dependence of the MSD (as shown in Fig. 4), whereas the difference among them are conspicuously revealed in the time-dependence of the kurtosis as can be appreciated in Fig. 5. The model proposed here is qualitatively most similar to the RTM model than to the ABP model, this, due to the manner how the memory function is damped out. It may be possible that if we modify the memory function in order to damped it out even more slowly, then we may get a dynamics closer to the ABP one, this is related to the fact that the higher hydrodynamic tensors, like $\mathbb{Q}_{ij}$, are damped out faster with time in the ABP model than as the RTM model does.

Our approach can be extended in various directions. For instance, the active particles under an external field can be treated directly by adding an extra term in the current probability. In addition, the effects of spatial heterogeneity on the dynamics of the active particle, such as when the particle motion occurs on a curved surface, can be immediately generalized for the GABM. Moreover, as we mentioned above, the memory function can be adjusted in order to capture different active behaviors. For example, we can modify the time dependence of the memory function in order to damped it out slower than the function proposed here. Also, the memory function can be modified to take into account a space dependence

to describe additional effects of spatial inhomogeneities. Furthermore, we can use the space dependence of the memory function to interpret it as a generalized diffusion process in order to treat the problem of the interacting active particle system within the context of the hydrodynamic fluctuation theory [14, 24].

ACKNOWLEDGMENTS

The authors kindly acknowledge support from DGAPA-UNAM PAPIIT-IN114717. PCV acknowledges financial support by CONACyT Grant No. 237425 and PROFOCIE-UNACH 2016 and 2017.

Appendix A: Alternative expressions for MSD and Kurtosis

In this section, we give the expressions for the mean-squared displacement and fourth moment directly from the probability distribution function (14). In the case of MSD one get

$$\langle \boldsymbol{x}^2(t)\rangle_{\rm a} = 2d\left[\frac{c^2}{\Gamma}t - \eta e^{-\Gamma t}\sum_{k=1}^{\infty}\frac{(\Gamma t)^k}{k!}\left[\psi(\eta+k)-\psi(\eta)\right]\right], \tag{A1}$$

where $\psi(x) = d\log\Gamma(x)/dx$ is the digamma function. The appearance of the exponential factor in front of the sum makes expression (A1) useful to determine the asymptotic regime, to say, $\langle \boldsymbol{x}^2\rangle_{\rm a} \simeq 2d\, D_{\rm eff} t$, which is the standard expression in the diffusive regime, where the effective diffusion constant is given by $D_{\rm eff} = c^2/\Gamma$. In addition, we got the following expression for the time dependence of the fourth moment

$$\begin{aligned}\langle \boldsymbol{x}^4(t)\rangle_{\rm a} = \frac{d(d+2)c^4}{\Gamma^4}\Big\{&-8\Gamma t + 4\Gamma^2 t^2 \\ &+ 8(\Gamma t+3)\eta\, e^{-\Gamma t}\sum_{k=1}^{\infty}\frac{(\Gamma t)^k}{k!}\left(\psi(\eta+k)-\psi(\eta)\right) \\ &- 16\eta\,\Gamma t e^{-\Gamma t}\sum_{k=1}^{\infty}\frac{(\Gamma t)^{k-1}}{(k-1)!}\left(\psi(\eta+k)-\psi(\eta)\right) \\ &+ 4\eta^2 e^{-\Gamma t}\sum_{k=1}^{\infty}\frac{(\Gamma t)^k}{k!}\left(\psi(\eta+k)-\psi(\eta)\right)^2\Big] \\ &+ 4\eta^2 e^{-\Gamma t}\sum_{k=1}^{\infty}\frac{(\Gamma t)^k}{k!}\left(\zeta(2,\eta+k)-\zeta(2,\eta)\right)\Big\},\end{aligned} \tag{A2}$$

where $\zeta(a,x)$ is the Hurwitz zeta function [21]. The kurtosis $\kappa_{\rm a}$ is obtained from last expression after dividing by $\langle \boldsymbol{x}^2(t)\rangle_{\rm a}^2$ and multiply by d^2. Clearly, the exponential prefactor in front of the sums appearing in equation (A2) allows us to identify immediately the asymptotic behavior of the kurtosis. Indeed, in this long-time limit, $\Gamma t \gg 1$, the fourth moment goes with time as $\langle \boldsymbol{x}^4(t)\rangle_{\rm a} \simeq 4d(d+2)c^4t^2/\Gamma^2$, and the mean-squared displacement as $\langle \boldsymbol{x}^2\rangle_{\rm a} = 2dc^2t/\Gamma$, thus the kurtosis has the constant value $\kappa_\infty \simeq d(d+2)$ as was previously anticipated in the former sections.

Appendix B: Hierarchy equations for active Brownian particles and run-and-tumble particles

The hydrodynamic tensor fields mentioned in section III are defined as follows

$$\rho(\boldsymbol{x},t) \equiv \int d\hat{\boldsymbol{v}}\; P(\boldsymbol{x},\hat{\boldsymbol{v}},t), \tag{B1a}$$

$$\mathbb{P}^i(\boldsymbol{x},t) \equiv \int d\hat{\boldsymbol{v}}\; \hat{\boldsymbol{v}}^i P(\boldsymbol{x},\hat{\boldsymbol{v}},t), \tag{B1b}$$

$$\mathbb{Q}^{ij}(\boldsymbol{x},t) \equiv \int d\hat{\boldsymbol{v}}\left(\hat{\boldsymbol{v}}^i\hat{\boldsymbol{v}}^j - \frac{\delta^{ij}}{d}\right)P(\boldsymbol{x},\hat{\boldsymbol{v}},t), \tag{B1c}$$

$$\mathbb{R}_{ijk}(\boldsymbol{x},t) \equiv \int d\hat{\boldsymbol{v}}\left(\hat{\boldsymbol{v}}^i\hat{\boldsymbol{v}}^j\hat{\boldsymbol{v}}^k - \frac{1}{d+2}\delta^{[ij}\hat{\boldsymbol{v}}^{k]_{\rm S}}\right)P(\boldsymbol{x},\hat{\boldsymbol{v}},t), \tag{B1d}$$

where $[\cdots]_{\rm S}$ indicates that the total symmetrization of the indices must be taken into account and $P(\boldsymbol{x},\hat{\boldsymbol{v}},t)$ is either $P_{\rm ABP}(\boldsymbol{x},\hat{\boldsymbol{v}},t)$ or $P_{\rm RTP}(\boldsymbol{x},\hat{\boldsymbol{v}},t)$.

After these definitions, we are going to determine the hierarchy of hydrodynamic equations for both models (24) and (25), respectively. The evolution equations (26),(27), (29) for $\rho(\boldsymbol{x},t)$, $\mathbb{P}^i(\boldsymbol{x},t)$, $\mathbb{Q}_{ij}(\boldsymbol{x},t)$, respecively, and so on, are obtained multiplying each equation (24) and (25) with each term of the orthogonal basis

$$\mathcal{B} = \left\{\mathbf{1}, \hat{\boldsymbol{v}}_i, \hat{\boldsymbol{v}}_i\hat{\boldsymbol{v}}_j - \frac{\delta_{ij}}{d}, \hat{\boldsymbol{v}}^i\hat{\boldsymbol{v}}^j\hat{\boldsymbol{v}}^k - \frac{1}{d+2}\delta^{[ij}\hat{\boldsymbol{v}}^{k]_{\rm S}}, \cdots\right\}, \tag{B2}$$

respectively, and integrated out the $\hat{\boldsymbol{v}}$ degrees of freedom. In order to implement this procedure for the ABPs case we notice that it is necessary to calculate the action of $\nabla^2_{\hat{v}}$ on each element of the basis $\mathcal{B}$. For these calculations we found useful to apply the Weingarten-Gauss (WG) structure equations, $\boldsymbol{\nabla}_a\mathbf{e}^b = -K_a^b\mathbf{n}$ and $\boldsymbol{\nabla}_a\mathbf{n} = K_{ab}\mathbf{e}^b$ valid for any hypersurface embedded in $\mathbb{R}^d$ of codimension 1, where $\boldsymbol{\nabla}_a$ is the covariant derivative compatible with the metric tensor g_{ab}, K_{ab} are the components of the extrinsic curvature tensor, $\{\mathbf{e}_a\}$ is a set of tangent vectors, and $\mathbf{n}$ is a normal vector at a point in the hypersurface [25]. In the case of the hypersphere S^{d-1} one has $\mathbf{n} = \hat{\boldsymbol{v}}$, $K_{ab} = g_{ab}$, and $\nabla^2_{\hat{v}} = \boldsymbol{\nabla}^a\boldsymbol{\nabla}_a$. For instance, the calculation $\nabla^2_{\hat{v}}\hat{\boldsymbol{v}}$ can be carried out using the WG Eqs. as $\nabla^2_{\hat{v}}\hat{\boldsymbol{v}} = \nabla^c\nabla_c\mathbf{n} = -g_{cb}g^{cb}\mathbf{n} = -(d-1)\hat{\boldsymbol{v}}$; similarly one can compute the Laplacian of the rest of the orthogonal basis terms. For the RTPs equations we found useful to apply the property that the integration $\int d\hat{\boldsymbol{v}}\;\cdot$ of each element of $\mathcal{B}$ is zero as a consequence of the compactness of S^{d-1}.

Next, we are going to sketch briefly the procedure used to obtain the mean-squared displacement (MSD) and the fourth moment for both ABPs and RTPs models. In particular, using the hierarchy equations shown above we are able to provide exact results for the mean-squared displacement and the fourth moment for both models. In particular for the MSD, one can obtain the equation using Eq. (28)

$$\frac{d^2}{dt^2}\left\langle \boldsymbol{x}^2(t)\right\rangle + \xi\frac{d}{dt}\left\langle \boldsymbol{x}^2(t)\right\rangle = \frac{v_0^2}{d} \times \int d^d\boldsymbol{x}\ \boldsymbol{x}^2\left[\nabla^2\rho + v_0^2\partial_i\partial_j\mathbb{Q}^{ij}\right]. \tag{B3}$$

Now, we perform an integration by parts and we use the traceless property of $\mathbb{Q}^{ij}$, therefore one obtain the ordinary differential equation for $\left\langle \boldsymbol{x}^2(t)\right\rangle$

$$\frac{d^2}{dt^2}\left\langle \boldsymbol{x}^2(t)\right\rangle + \xi\frac{d}{dt}\left\langle \boldsymbol{x}^2(t)\right\rangle = 2v_0^2. \tag{B4}$$

Under the initial conditions $\left\langle \boldsymbol{x}^2(t)\right\rangle = 0$ and $d\left\langle \boldsymbol{x}^2(t)\right\rangle/dt = 0$ at $t = 0$, one can get easily the MSD

$$\langle \boldsymbol{x}^2(t)\rangle = \frac{2v_0^2}{\xi^2}\left[\xi t - (1-e^{-\xi t})\right], \tag{B5}$$

where we recall that $\xi = (d-1)D_{\mathrm{R}}$ and $\xi = \lambda$ for ABPs and RTPs models, respectively. It is noteworthy to mention that the RTPs mean-squared displacement does not depend on the dimension d of the space.

Next, we are going to calculate the fourth moment of the ABPs model. The procedure implemented is similar to the one uses for the MSD. Using Eq. (28) one is able to obtain the following differential equation

$$\frac{d^2}{dt^2}\left\langle \boldsymbol{x}^4(t)\right\rangle + \xi\frac{d}{dt}\left\langle \boldsymbol{x}^4(t)\right\rangle = \frac{4v_0^2(d+2)}{d}\left\langle \boldsymbol{x}^2(t)\right\rangle + 8v_0^2\mathcal{J}(t) \tag{B6}$$

where

$$\mathcal{J}(t) \equiv \int d^d\boldsymbol{x}\ x_i x_j\mathbb{Q}^{ij}(\boldsymbol{x},t). \tag{B7}$$

This quantity can be determined using the equations of the hierarchy. In particular, using Eq. (29), and the traceless property of $\mathbb{R}^{ijk}$ one is able to find the equation

$$\frac{d\mathcal{J}}{dt} = -\bar{\xi}\mathcal{J} - \frac{v_0}{d+2}\mathcal{K}(t) \tag{B8}$$

where we recall the values of $\bar{\xi}$ for ABPs and RTPs models, respectively, and $\mathcal{K}(t)$ is given by

$$\mathcal{K}(t) = \int d^d\boldsymbol{x}\ x_i x_j\mathbb{T}^{ij}(\boldsymbol{x},t). \tag{B9}$$

This quantity can be simplify using the structure of the tensor $\mathbb{T}^{ij}(\boldsymbol{x},t)$ and integrating by parts, thus one get $\mathcal{K}(t) = -2(d+2)(d-1)\mathcal{L}(t)/d$, where $\mathcal{L}(t)$ is given by

$$\mathcal{L}(t) = \int d^d\boldsymbol{x}\ x_i\mathbb{P}^i(\boldsymbol{x},t). \tag{B10}$$

Using the Eq. (27) and the identity $e^{-\xi t}d(e^{\xi t}v)/dt = dv/dt + \xi v$, one is able to find the following ordinary differential equation $e^{-\xi t}d/dt\left(e^{\xi t}\mathcal{L}\right) = v_0$ Under the initial condition $\mathcal{L}(0) = 0$, one can get easily the following solution

$$\mathcal{L}(t) = \frac{v_0}{\xi}\left(1-e^{-\xi t}\right). \tag{B11}$$

Finally, using the expression for $\mathcal{L}(t)$ we get an expression for $\mathcal{K}(t)$, and then substitute it in Eq. (B8) in order to determine $\mathcal{J}(t)$. Here, we also use the identity

$$e^{-\xi t}\frac{d}{dt}(e^{\xi t}v) = \frac{dv}{dt} + \xi v. \tag{B12}$$

In particular, the equation for $\mathcal{J}(t)$ is then given by

$$e^{-\bar{\xi}t}\frac{d}{dt}\left(e^{\bar{\xi}t}\mathcal{J}(t)\right) = \frac{2v_0^2(d-1)}{d\xi}\left(1-e^{-\xi t}\right). \tag{B13}$$

Now, we solve this equation for the initial condition $\mathcal{J}(0) = 0$, then one have

$$\mathcal{J}(t) = \frac{2(d-1)v_0^2}{d\bar{\xi}\xi(\xi-\bar{\xi})}\left(\xi - \bar{\xi} + \bar{\xi}e^{-\xi t} - \xi e^{-\bar{\xi}t}\right). \tag{B14}$$

The $\mathcal{J}(t)$ solution is therefore substituted in Eq. (B6) in order to determine the fourth moment $\left\langle \boldsymbol{x}^4\right\rangle$. In addition, using the identity (B12), one is able to show that Eq. (B6) turns out to be

$$e^{\xi t}\frac{d}{dt}\left[e^{\xi t}\frac{d}{dt}\left\langle \boldsymbol{x}^4(t)\right\rangle\right] = \frac{8v_0^4(d+2)}{d\xi^2}\left[\xi t - (1-e^{-\xi t})\right] + \frac{16(d-1)v_0^4}{d\bar{\xi}\xi(\xi-\bar{\xi})}\left(\xi - \bar{\xi} + \bar{\xi}e^{-\xi t} - \xi e^{-\bar{\xi}t}\right) \tag{B15}$$

Under the initial conditions $\left\langle \boldsymbol{x}^4(t)\right\rangle = 0$ and $d\left\langle \boldsymbol{x}^4(t)\right\rangle/dt = 0$ at the time $t = 0$, the solution of the last differential equation (B15) is given by

$$\langle \boldsymbol{x}^4(t)\rangle = \frac{4v_0^4}{d\xi^4\bar{\xi}^2(\xi-\bar{\xi})^2}\Big[4(d-1)\xi^4e^{-\bar{\xi}t} - 2\bar{\xi}^2e^{-\xi t}\left(3d\xi^2(\xi t+3) + (d+2)\bar{\xi}^2(\xi t+3) - 2\xi\bar{\xi}(d(2\xi t+5) + \xi t + 4)\right) + (\xi-\bar{\xi})^2\left(-4(d-1)\xi^2 + (d+2)\bar{\xi}^2(\xi t(\xi t-4)+6) + 4(d-1)\xi\bar{\xi}(\xi t-2)\right)\Big]. \tag{B16}$$

In particular, we should take carefully the limit $\xi \to \overline{\xi} = \lambda$ for the RTPs model, which leads to the expression

$$\langle \boldsymbol{x}^4(t)\rangle = \frac{4v_0^4}{d\lambda^4}\Big\{6(d-4)e^{-\lambda t} + 6(d-2)t\lambda e^{-\lambda t} + 2(d-1)t^2\lambda^2 e^{-\lambda t} + \Big((d+2)t^2\lambda^2 - 12t\lambda - 6(d-4)\Big)\Big\}. \quad \text{(B17)}$$

The behavior of the fourth moment for both models at the short-time regime is $\langle \boldsymbol{x}^4(t)\rangle \simeq v_0^4 t^4$.

[1] S. Goldstein, The Quarterly Journal of Mechanics and Applied Mathematics **4**, 129 (1951), http://qjmam.oxfordjournals.org/content/4/2/129.full.pdf+html, URL http://qjmam.oxfordjournals.org/content/4/2/129.abstract.

[2] F. J. Sevilla and M. Sandoval, Phys. Rev. E **91**, 052150 (2015), URL http://link.aps.org/doi/10.1103/PhysRevE.91.052150.

[3] F. J. Sevilla, Phys. Rev. E **94**, 062120 (2016), URL http://link.aps.org/doi/10.1103/PhysRevE.94.062120.

[4] P. Castro-Villarreal and F. J. Sevilla, Phys. Rev. E **97**, 052605 (2018), URL https://link.aps.org/doi/10.1103/PhysRevE.97.052605.

[5] L. Apaza and M. Sandoval, Soft Matter **14**, 9928 (2018), URL http://dx.doi.org/10.1039/C8SM01034J.

[6] F. Schweitzer, *Brownian agents and active particles: collective dynamics in the natural and social sciences* (Springer, 2007).

[7] Kurzthaler Christina, Leitmann Sebastian, and Franosch Thomas, Scientific Reports **6**, 36702 (2016).

[8] K. Martens, L. Angelani, R. Di Leonardo, and L. Bocquet, The European Physical Journal E **35**, 84 (2012), ISSN 1292-895X, URL https://doi.org/10.1140/epje/i2012-12084-y.

[9] F. J. Sevilla and L. A. Gomez Nava, Physical Review E **90**, 022130 (2014).

[10] J. M. Porra, J. Masoliver, and G. H. Weiss, Physical Review E **55**, 7771 (1997).

[11] C. Kurzthaler, C. Devailly, J. Arlt, T. Franosch, W. C. Poon, V. A. Martinez, and A. T. Brown, arXiv preprint arXiv:1712.03097 (2017).

[12] F. J. Sevilla, *The Non-equilibrium Nature of Active Motion* (Springer International Publishing, Cham, 2018), pp. 59–86, ISBN 978-3-319-73975-5, URL https://doi.org/10.1007/978-3-319-73975-5_4.

[13] F. J. Sevilla, R. F. Rodríguez, and J. R. Gomez-Solano, Phys. Rev. E **100**, 032123 (2019), URL https://link.aps.org/doi/10.1103/PhysRevE.100.032123.

[14] Forster D., *Hydrodynamic fluctuations, broken symmetry, and correlation functions* (W. A. Benjamin, Inc., Reading, MA, 1975), URL https://www.osti.gov/servlets/purl/4185024.

[15] F. J. Sevilla, arXiv:1905.07090 [cond-mat.stat-mech] (2019).

[16] V. Kenkre and F. J. Sevilla, in *Contributions to Mathematical Physics: a Tribute to Gerard G. Emch TS. Ali, KB. Sinha, eds.* (Hindustan Book Age ncy, New Delhi, 2007), pp. 147–160.

[17] J. Dunkel and P. Hnggi, Physics Reports **471**, 1 (2009), ISSN 0370-1573, URL http://www.sciencedirect.com/science/article/pii/S0370157308004171.

[18] M. E. Cates and J. Tailleur, EPL (Europhysics Letters) **101**, 20010 (2013), URL http://stacks.iop.org/0295-5075/101/i=2/a=20010.

[19] W. Bietenholz and J. J. Giambiagi, J. Math. Phys. **36**, 383 (1995).

[20] C. Kurzthaler, C. Devailly, J. Arlt, T. Franosch, W. C. K. Poon, V. A. Martinez, and A. T. Brown, Phys. Rev. Lett. **121**, 078001 (2018), URL https://link.aps.org/doi/10.1103/PhysRevLett.121.078001.

[21] M. Abramowitz and I. A. Stegun, *Handbook of Mathematical Functions with Formulas, Graphs, and Mathematical Tables* (Dover, New York, 1964), ninth dover printing, tenth gpo printing ed., ISBN 0-486-61272-4.

[22] J. D. Barrow, Philosophical Transactions of the Royal Society of London. Series A, Mathematical and Physical Sciences **310**, 337 (1983).

[23] K. V. Mardia, Sankhyā: The Indian Journal of Statistics, Series B pp. 115–128 (1974).

[24] W. Hess and R. Klein, Advances in Physics **32**, 173 (1983), URL https://doi.org/10.1080/00018738300101551.

[25] S. Montiel and A. Ros, *Curves and surfaces*, vol. 69 (American Mathematical Soc., 2009).